A HIGH STABILITY INTENSITY MONITORING SYSTEM FOR THE ISIS EXTRACTED PROTON BEAM

Michael A. Clarke-Gayther, RAL, Didcot, United Kingdom

ABSTRACT

A description is given of the extracted proton beam intensity monitoring system on the high intensity pulsed neutron source, ISIS, at the Rutherford Appleton Laboratory. The system, consisting of six resonant mode toroidal beam current monitors, and signal conditioning electronics, measures protons per pulse in the range 2e10-4e13 p.p.p. with good linearity, and has shown excellent long term stability.

1 INTRODUCTION

The non-destructive, accurate, and stable measurement of beam intensity is an important diagnostic requirement at particle accelerators. Measurement systems, based on toroidal beam current transformers [1], where the charged particle beam, and its image (wall) current form a single turn primary winding, are in widespread use, and have been the subject of continuous development [2]. High accuracy AC, DC, and DC to wide-band beam transformers are now commercially available [3]. Systems can be configured to provide information on: the time dependent variation of beam current (current viewing); the instantaneous beam current (sampled); the average beam current; and the beam charge (charge per pulse). Processed measurements yield data on accelerator system efficiencies (e.g. at injection, acceleration or extraction), and beam loss.

Accurate measurement of beam charge for beam pulse durations in the 1e-8 to 1e-5 (s) range has been demonstrated by systems using integrating resonant mode beam transformers [4,5]. A system of this type, consisting of six resonant mode toroidal beam current transformers, and signal conditioning electronics, measures protons per pulse, in the extracted proton beam at ISIS.

2 THEORY OF OPERATION

The equivalent circuit for the generalised beam current transformer is shown in fig.1. The pulsed beam current I_B and its image (wall) current form a single turn primary winding, inducing a magnetic flux Φ in the core and a voltage V_S across the secondary winding. The high permeability toroidal core ensures tight magnetic coupling (k=1) between the primary and secondary windings.

Where: $V_S = -kn\dot{\Phi} = -knL_0\dot{I}_P = -kL_S\dot{I}_P/n$ is Faraday's law, $I_p = I_B$, and L_0 ,L_S , R, C, and n, represent the single turn inductance, the total secondary inductance, the total losses, the secondary load capacitance and the number of secondary turns.

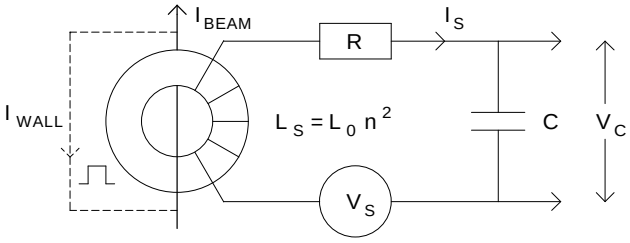

Figure 1: Equivalent circuit of beam current transformer

The voltage loop equation, describing the transfer function of the equivalent circuit, is given by:

$$L_S\dot{I}_S + RI_S + Q_C/C = -kn\dot{\Phi} = -kL_S\dot{I}_P/n$$

with the general solution of the homogeneous equation given by:

$$I(t) = c_1e^{-\lambda_1 t} + c_2e^{-\lambda_2 t}, \quad \lambda_{1,2} = \frac{R}{2L_S} \pm \sqrt{\frac{R^2}{4L_S^2} - \frac{1}{L_SC}}$$

There are two important cases:

1. When: $\frac{R^2}{4L_S^2} - \frac{1}{L_SC} > 0$, (overdamped response)

λ_1 and λ_2 are real, and the response is that of the simple current transformer, with a time constant $\tau = L_S/R$, and where $I_S = I_B /n$. Electronic integration of I_S can provide a measure of charge, but this process can be inaccurate for short pulses.

2. When: $\frac{R^2}{4L_S^2} - \frac{1}{L_SC} < 0$, (underdamped response)

λ_1 and λ_2 are complex, and the response is that of the resonant mode transformer, where the secondary current charges load capacitor C during the beam pulse, and initiates a damped oscillation at the natural resonant frequency ω_0 of the LCR network. The amplitude of the oscillation, sampled as the voltage developed across C, can be shown to be proportional to beam pulse charge. This relationship is explored, without loss of generality, by analysing the solution of the loop equation for a gate function beam current pulse of duration T.

Where: $I_p(t) = I_B$ for $0 \le t \le T$
and, $I_p(t) = 0$ for $t > T$,

the exact solution for V_C (t) can be shown [5] to be given by the sum of two exponentially decaying sine functions, initiated at t = 0 , and at t = T, respectively, as shown in fig.2, giving:

$$V_C(t) = -\frac{I_B}{n\omega_0 C} e^{-\lambda t}\left[(\sin\omega_0 t) - (e^{\lambda T}\sin\omega_0(t-T)_{t\geq T})\right]$$

where the resonant frequency: $\omega_0 = \sqrt{\frac{1}{L_S C} - \frac{R^2}{4L_S^2}}$

and the decay time constant: $1/\lambda = 2L_S/R$

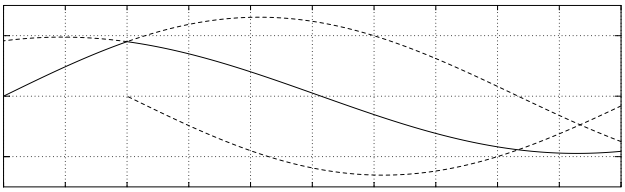

Figure 2: Exact solution functions for V_C (t)

As T→0 $\quad V_C(t) \approx \frac{-2I_B}{n\omega_0 C}(e^{-\lambda t}\cos\omega_0 t)$

and for T>0, and $\lambda < 0.01\omega_0$ the following simplified equation gives a value for V_C(t) that is in error by < 0.01% of the exact solution:

$$V_C(t) \approx \frac{-2I_B}{n\omega_0 C}\left[\sin\frac{\omega_0 T}{2}\right]\left[e^{-\lambda(t-T/2)}\right]\left[\cos\omega_0\left(t-\frac{T}{2}\right)\right]$$

For $\omega_0 T < 1, \quad \sin\omega_0 T \approx (\omega_0 T/2 - {\omega_0}^3 T^3/3!2^3)$

$$V_C(t) \approx \frac{-I_B T}{nC}\left[1-\frac{{\omega_0}^2 T^2}{24}\right]\left[e^{-\lambda(t-T/2)}\right]\left[\cos\omega_0\left(t-\frac{T}{2}\right)\right]$$

where the terms in brackets are due to: integration error, damping, and waveform function, respectively. For beam pulse durations in the range $0 < T \leq T_{MAX}$ the magnitude of the corresponding integration error Δ (%) is determined by the resonant frequency ω_0 , where: $\Delta(\%) = ({\omega_0}^2 T^2/24)\ 100$.

Finally, if V_C is sampled at $t = ((\pi/\omega_0) + T/2)$, and the beam pulse duration (T) is a constant (as is the extracted beam pulse at ISIS), the contributions from the pulse duration dependant terms can be combined giving:

$$V_C(t) \approx \frac{I_B T}{nC}(A) \approx \frac{Q_B}{nC}(A)$$

Where Q_B is the total beam pulse charge, and A is a unique calibration constant, determined for each channel.

3 MECHANICAL DESIGN FEATURES

The mechanical construction of the resonant mode current transformer is shown in fig.3. This UHV compatible, radiation hard design, occupies a minimum beamline length, and utilises an ex-RF cavity, nickel-zinc ferrite core (μ_R = 180), with a 50 turn, centre tapped secondary winding. A nickel plated steel casing, with an internal mumetal screen provide isolation from interfering magnetic and electric fields. The precision (NPO) ceramic chip, load capacitor(s) [6] are mounted on a plug in printed circuit board that can be easily removed for measurement purposes. The housing is fitted with 'quick release' vacuum, and mounting clamps, to facilitate efficient 'hands on' maintenance.

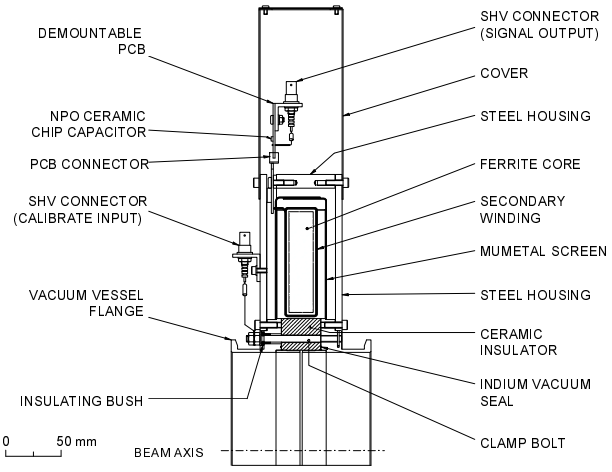

Figure 3: Beam transformer construction

4 ELECTRONIC SYSTEM DESIGN

The important features of the signal conditioning and data acquisition system are shown in fig.4. Values for the secondary inductance (L_S), number of turns (n), and load capacitance (C), were chosen to give an

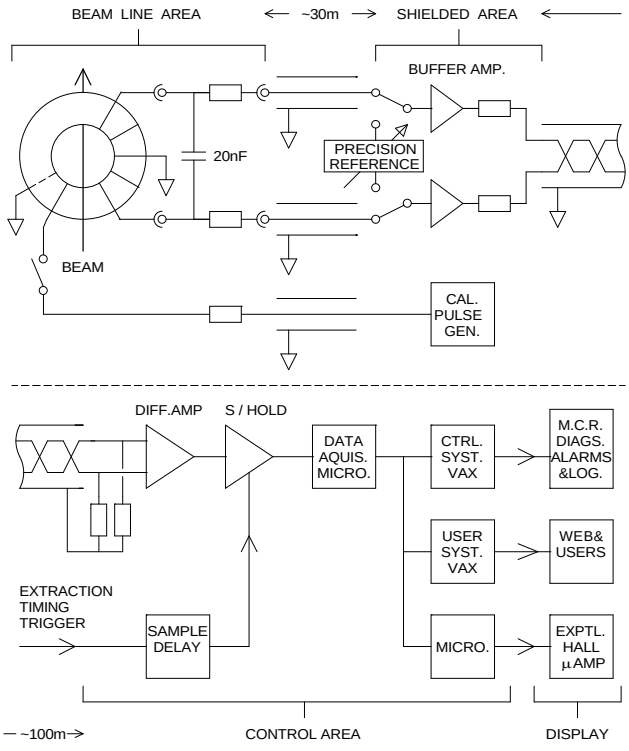

Figure 4: Electronic system schematic

acceptable compromise between signal amplitude, frequency ($\omega_0 / 2\pi$), integration error (Δ), and damping factor (λ). The ISIS resonant mode beam transformers have the following design parameters:

ω_0 = 1.9e5 s^{-1}	n = 50	μ_R = 180
L_S = 1.4e-3 H	C = 2e-8 F	R = 1.8 Ω
Δ = 0.02 %	T = 4.0e-7 s	$1/\lambda$ = 1.5e-3 s

The secondary winding outputs a balanced differential signal, with a dynamic source impedance of ~ 40 kΩ, to a remote, high impedance buffer amplifier, via ~30 metres of low capacitance coaxial cable. The capacitance of this cable, forms part of the total load capacitance, and is included in the calculated channel calibration constant. The buffered, high level, low impedance signal, is output to a remote differential receiver amplifier, via ~100 metres of screened, twisted pair cable. A delayed timing pulse, synchronised to beam extraction, triggers a precision sample-hold circuit that subsequently acquires and stores the transformer signal, at peak amplitude, during the first cycle of oscillation. A schematic of the primary and secondary

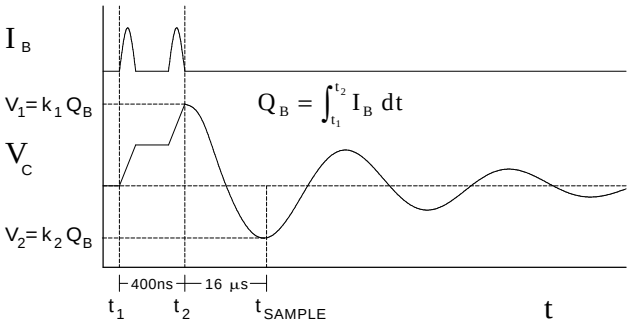

Figure 5: Waveform schematic

waveforms is shown in fig.5, where $V_C = V_1$ at the end of integration, and $V_C = V_2$ at the peak of the first maximum. The signal decays with a time constant of 1.5 ms (Q = 140), and drops to < 1e-6 of the initial value in the ISIS cycle time of 20 ms. The six sampled signals are digitised, and the resulting raw data is distributed to the display systems as shown in fig.4.

5 TEST SET-UP

The relationship between transformer primary charge, and secondary voltage was determined using the circuit shown in fig.6. The circuit simulates the ISIS extracted beam pulse. A charged line (Z_0 = 12.5 Ω), with a precisely determined electrical length (400ns), delivers a pulse with a programmable voltage amplitude in the range 0.1 ~ 100 V, to a precision high voltage, pulse rated termination [7], resulting in a primary charge pulse in the range 3e-9~3e-6 C. The secondary voltage waveform, sampled at the first maximum, divided by the primary pulse charge ($Q_P = V_L T_P / 2 Z_0$), yielded a

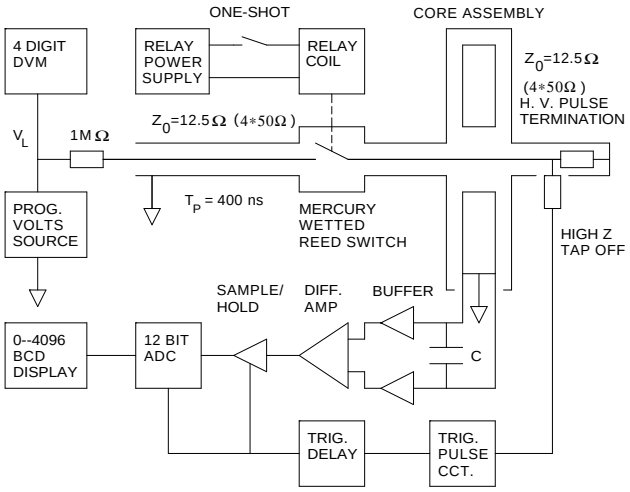

Figure 6: Test circuit schematic

measurement of non-linearity of ± 0.2% for primary charge in the range 3e-9~ 3e-6 C. The accuracy of calibration was estimated to be within 0.5 % of absolute.

6 OPERATIONAL EXPERIENCE

The resonant mode beam charge monitoring system has demonstrated excellent long term calibration stability. The calibration factors for the six transformers have changed by < ± 0.1% / year. The precision ceramic chip capacitors, have been measured at regular intervals, and show changes in value of < ± 0.01% year, including, in one case, a component that has received an estimated accumulated radiation dose of between 3e5 and 5e5 Gy.

7 ACKNOWLEDGEMENT

Contributions from the following are gratefully acknowledged. A. Borden, and D. Wright (data acquisition microcomputer, software and display), R. Steiner (helpful comments), M. Southern (mechanical design), ISIS Controls group (display hardware and software), and many others.

REFERENCES

[1] Robert C. Webber, 'Charged Particle Beam Current Monitoring', AIP conf. proc. No.333 (1995), p.3-23.
[2] Klaus B. Unser, 'Recent advances in beam current transformer technology', Proc. of first European workshop on beam diagnostics, Montreux, Switzerland, May 1993, p.105-109.
[3] Julien Bergoz,'Current monitors for particle beams', Nuclear Physics, A525 (1991), p.595c-600c.
[4] R. Steiner, K. Merle and H. G. Andresen, 'A high-precision ferrite-induction beam-current monitoring system', Nucl. Instr.and Meth. 127 (1975), p.11-15.
[5] R. S. Larsen and D.Horelick, 'A precision toroidal charge monitor for SLAC', SLAC-PUB-398 (1968).
[6] Vitramon Ltd, High Wycombe, Bucks., UK.
[7] Barth Electronics Inc., Boulder City, Nevada, USA.